

## **Supplemental material**

### **1. Supplementary Methods**

#### **1.1. Samples**

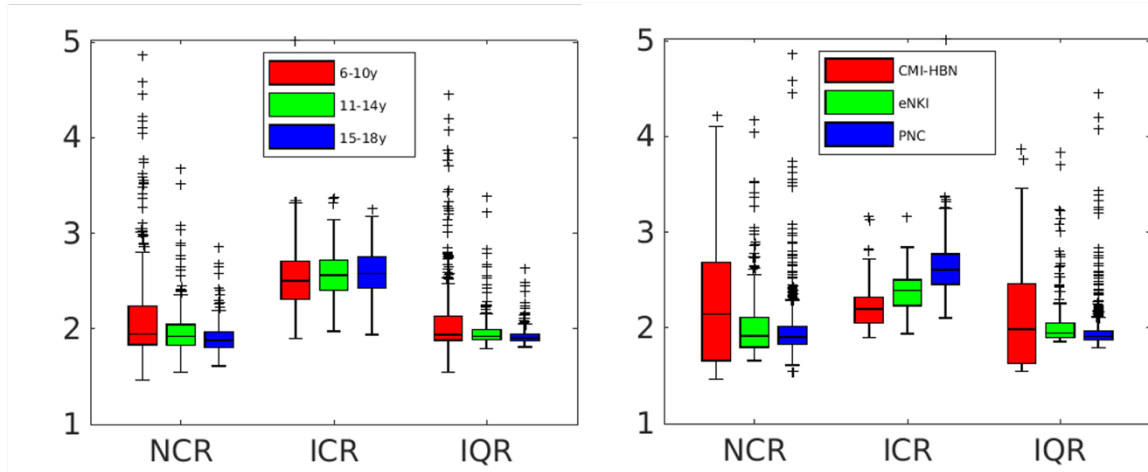
Scanning parameters of the eNKI, PNC and CMI-HBN datasets are summarized in Tab. 1.

Table 1. Scanning parameters of age-cohort samples

| Dataset | Sequence parameters  |
|---------|--|
| eNKI    | Lifespan Connectomics and Longitudinal Developmental Connectomics study: T1 (3D-MPRAGE), Tim Trio, 176, TR= 1900 ms, TE = 2.52 ms, TI= 900 ms, FoV = 250 x 250 mm <sup>2</sup> , flip angle = 9°, voxel size = 1 x 1 x 1 mm <sup>3</sup> ; Neurofeedback study: T1 (3D-MPRAGE), Tim Trio, 192 slices, TR = 2600 ms, TE = 3.02 ms, TI = 900 ms, flip angle = 8°, voxel size = 1 x 1 x 1 mm <sup>3</sup> |
| PNC     | 3T Siemens Tim Trio, 3D-MPRAGE, TR=1810 ms, TE = 3.5 ms, TI = 1100 ms, FoV = 180 x 240 mm, Flip angle = 9°, voxel size = 1 x 1 x 1 mm <sup>3</sup>   |
| CMI-HBN | 3T Siemens Tim Trio, 3D MPRAGE, FoV Phase = 100 %, TR = 2500 ms, TE = 3.15 ms, TI = 1060 ms, flip angle = 8°, voxel size = 0.8 x 0.8 x 0.8 mm <sup>3</sup> ; 3T Siemens Prisma, 3D MPRAGE, FOV Phase = 100 %, TR = 2500 ms, TE = 3.15 ms, TI = 1060 ms, flip angle = 8°, voxel size = 1.0 x 1.0 x 1.0 mm <sup>3</sup>  |

#### **1.2 Quality assurance**

The quality assurance check in SPM12 revealed an overall good quality of MRI images (Fig. 1). Age-cohort samples were comparable in their quality ratings even though CMI-HBN dataset revealed a slightly higher variance in image quality.



**Figure 1.** Quality check of MRI images. *Note.* NCR = Noise Contrast Ratio, ICR = Inhomogeneity Contrast ratio, IQR = weighted average Image Quality Rating.

### 1.3 Grey matter volume differences of anterior and posterior hippocampal formation in childhood and adolescence

In addition to the examination of hippocampal differentiation patterns across age groups, we also investigated age effects on volumetric differences across age. Here, we used generalized additive models (GAM) to compute the relationship between age and grey matter volume controlling for total intracranial volume (TIV) and sex. The analysis was performed in Rstudio 1.2.5042 using the mgcv package (version 1.8-31). In the GAM model we used the smoothing terms ‘s’ to model age effects, with default penalizing parameters with five knots (k) representing the number of basis functions that were used to generate the smooth function. As a method we used restricted maximum likelihood (REML) to estimate the smoothing parameters. The estimated degrees of freedom (edf) defined the number of degrees of freedom that were used by the smooth function fitting the data. Edf values higher than one indicated that the fit to the data was non-linear representing more likely curvilinear relationships.

We computed a GAM model on the anterior and posterior subregions of the hippocampal differentiation pattern. First, as was described in the sections above we obtained an age specific hippocampal differentiation pattern for each age group separately. We then merged the age-specific patterns (e.g. 6-10 years, 11-14 years and 15-18 years) and applied bootstrapping to create a general, cross-age differentiation pattern of the most robust and consistent pattern based on our previously introduced criteria. This was done to overcome qualitative differences in differentiation patterns due to age. The final hippocampal differentiation pattern was a representation of the previous age specific hippocampal differentiation patterns (Fig. 5).

## **2. Supplementary Results**

### **2.1 Consistency within left hippocampal differentiation patterns**

The within hippocampal consistency assessed with the silhouette score confirmed in addition to the stability measures that basic patterns of 2 and 3 subregions are the most consistent divisions visualized with the silhouette plots (Fig. 2).

The assessment across age group consistency measured with the aRI revealed lower consistencies between divisions of higher levels such as 5-7 subregions (Fig. 2 B). But the age group specific differentiation pattern into 6 subregions achieved higher consistency across age groups indicating a potential reliable division to study age effects at higher levels of differentiation (Fig. 2 C).

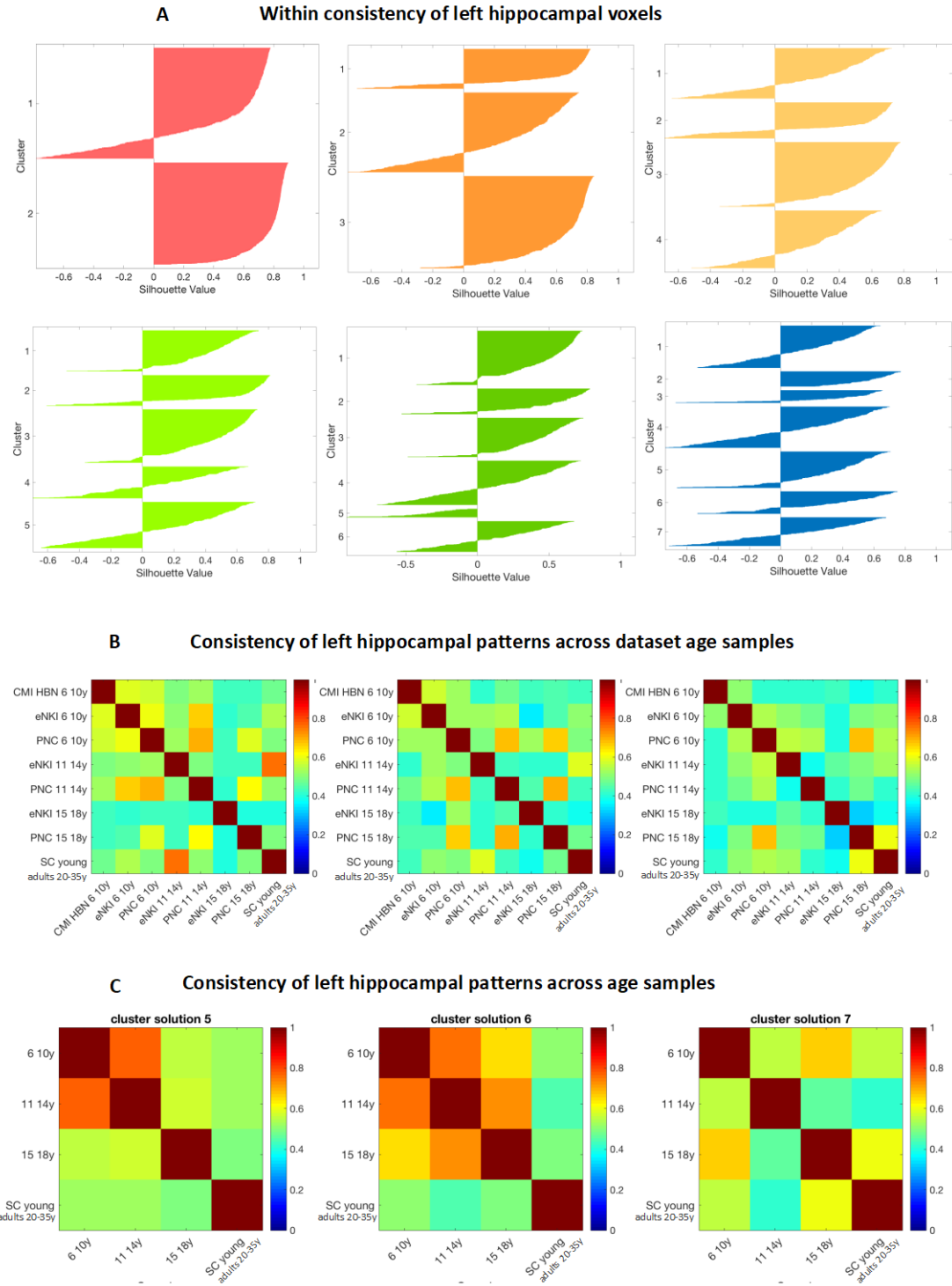


**Figure 2.** Consistency within differentiation patterns and across age samples for the left HS.

## 2.2 Stability of right hippocampal differentiation patterns

We performed a 6 (differentiation patterns: from 2 to 7) x 3 (age group: 6-10 years, 11-14 years, 15-18 years) ANOVA with the aRI as dependent variable measuring stability across 10 000 splits. All main and the interaction effects were significant for the right HS: differentiation patterns  $F(5,419982) = 15255.58$ ,  $P < 0.001$ , age group  $F(2,419982) = 8085.51$ ,  $P < 0.001$ , differentiation patterns x age group  $F(10,419982) = 4712.29$ ,  $P < 0.001$ . All post-hoc tests for multiple comparisons (Tukey-Kramer method) were significant comparing all differentiation patterns with each other: 2 ( $M = 0.96$ ), 3 ( $M = 0.92$ ), 4 ( $M = 0.92$ ), 5 ( $M = 0.90$ ), 6 ( $M = 0.87$ ), and 7 ( $M = 0.90$ ) (Fig. 3).

### **2.3 Consistency within the right hippocampal differentiation patterns and across dataset age groups**

We ran a 6 (differentiation pattern: 2-7) x 3 (age group: 6-10 years, 11-14 years, 15-18 years) ANOVA with the silhouette criterion as dependent variable for the right HS to assess hippocampal voxels' consistency. The results revealed that all main and the interaction effect were significant: differentiation pattern  $F(5,15552) = 563.16$ ,  $P < 0.001$ , age group  $F(2,15552) = 8.18$ ,  $P < 0.001$ , interaction between differentiation pattern x age group  $F(10,15552) = 11.86$ ,  $P < 0.001$ . Post-hoc comparisons of differentiation patterns for multiple comparisons (Tukey-Kramer) yielded that the silhouette values of simpler levels of differentiation (2 and 3 subregions) differed significantly when compared to all the other differentiation patterns (4-7) ( $P < 0.001$ ). But no significant differences in silhouette values were found if comparing differentiation patterns between 4 to 7 subregions ( $P > 0.43$ ), suggesting that no substantial difference in hippocampal consistency occurs if we increase the level of differentiation above three subregions. Silhouette plots for left and right hippocampal differentiation patterns are presented in Fig. 3 B/C.



**Figure 3.** Stability and consistency measure of right hippocampal differentiation patterns.

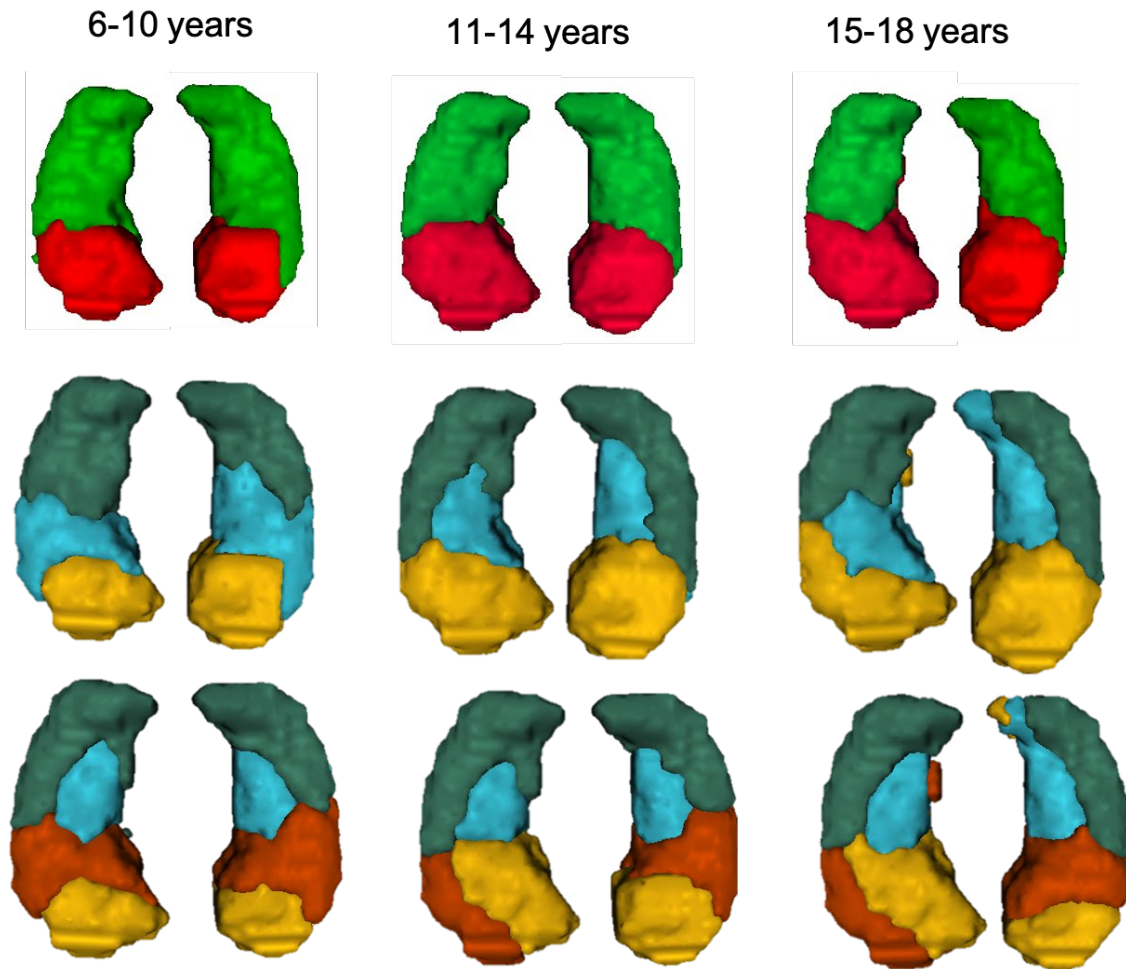


**Figure 4.** Age related hippocampal differentiation patterns of 2 to 4 subregions.

#### **2.4 Volumetric differences of anterior and posterior hippocampal formation in childhood and adolescence**

Anterior ( $\text{edf} = 2.87$ ,  $F = 29.05$ ,  $P < 0.001$ ) and posterior ( $\text{edf} = 3.60$ ,  $F = 31.13$ ,  $P < 0.001$ ) subregions of the left HS follow slightly different volumetric trajectories across age. Anterior and posterior subregions of the right HS follow more similar trajectories across age (anterior:  $\text{edf} = 3.37$ ,  $F = 25.96$ ,  $P < 0.001$ ; posterior:  $\text{edf} = 3.42$ ,  $F = 31.88$ ,  $P < 0.001$ ). The left anterior HS demonstrates a slightly linear decrease in volume until the age of 13 years, whereas the left

posterior HS shows a more curvilinear increase of volume around the age of 8-12 years (Fig. 5). In the right HS, the anterior and posterior subregions increase in volume around the age of 8-12 years, implying that this period of late childhood and early adolescence is accompanied by specific processes and changes that are probably related to the onset of puberty, hence influencing HS' volume.

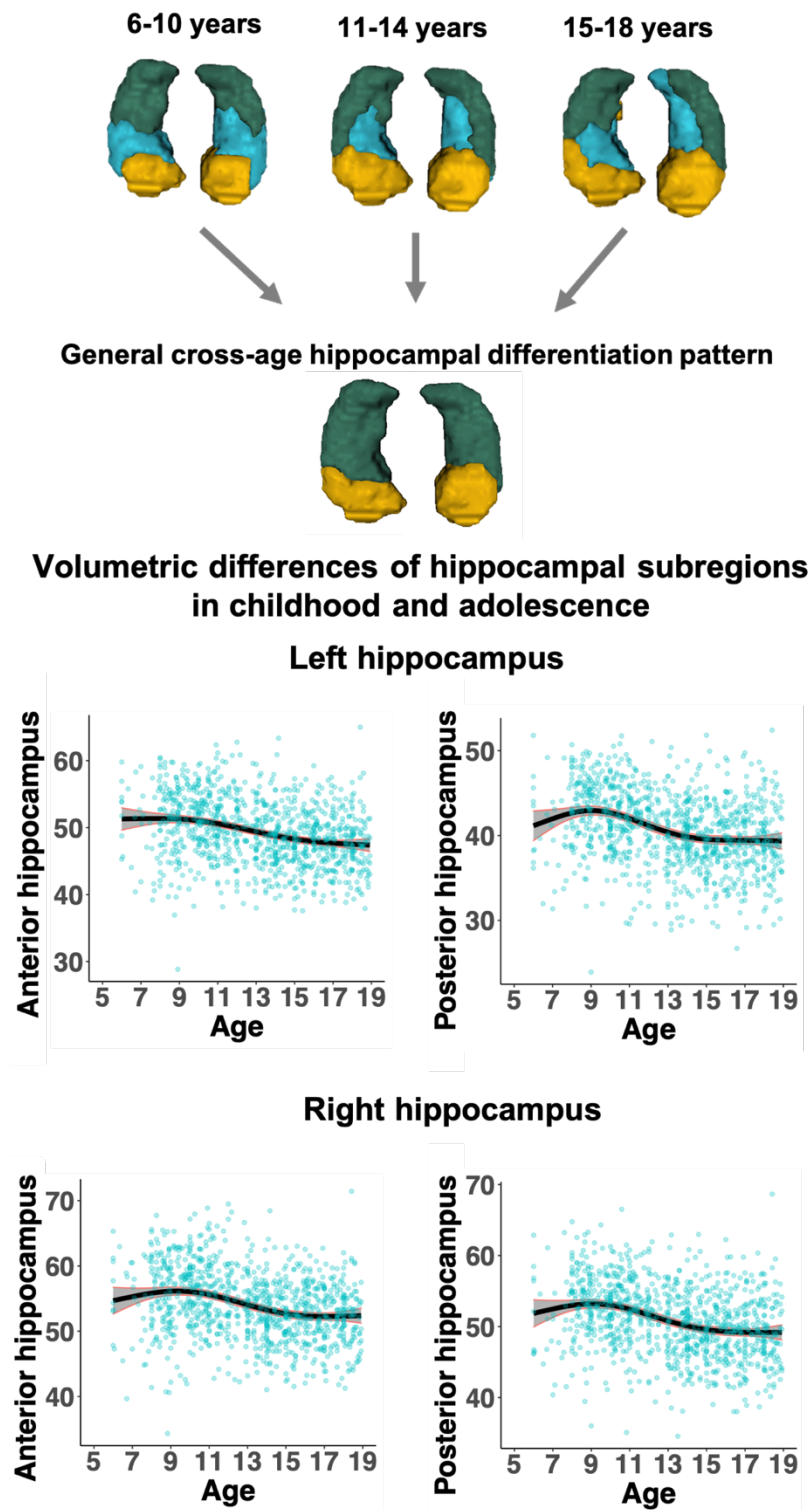




**Figure 5.** Volumetric differences in childhood and adolescence for anterior and posterior HS.

## **2.5 Structural covariance networks underlying right hippocampal differentiation pattern and their behavioral characterization**

Underlying structural covariance networks of right hippocampal subregions revealed that the anterior subregion covaried with almost the whole brain across late childhood and adolescence, with slight reductions in network expansion in higher age groups. The anterior hippocampal subregion was associated with frontal brain regions (frontal pole, superior, middle frontal gyrus, frontal orbital cortex, precentral gyrus, cingulate gyrus), temporal brain regions (temporal pole, planum polare, inferior temporal gyrus), subcortical regions (caudate, putamen, pallidum, amygdala), insular cortex, precuneous cortex, angular gyrus, lateral occipital cortex in late childhood. However, the structural covariance network was less expanded into the lingual gyrus, occipital pole, intracalcarine cortex, superior temporal gyrus and thalamus.

In early adolescence, the anterior hippocampal subregion was associated with the brain regions reported for late childhood, but also extended including the thalamus, insular cortex, cerebellum VI, Crus I, II, angular gyrus, and superior temporal gyrus. In middle adolescence, the associated structural covariance network was reduced from frontal regions except for the frontal pole, cingulate gyrus, superior frontal gyrus, inferior frontal gyrus (pars triangularis, pars opercularis), postcentral gyrus. However, the main clusters were temporally and posteriorly located, including temporal pole, inferior temporal gyrus, temporal occipital fusiform cortex. Associations were also found for intracalcarine cortex, lateral occipital cortex, occipital pole, precuneous cortex, cuneal cortex, thalamus.

The tail subregion of the right HS was associated with caudate, thalamus, pallidum, putamen, temporal occipital fusiform cortex, occipital pole, frontal pole, middle frontal gyrus, precentral gyrus, superior parietal lobule, lateral occipital cortex, supracalcarine cortex, angular gyrus, frontal operculum cortex, inferior frontal gyrus (pars opercularis, pars triangularis), frontal, lingual gyrus in the group of late childhood. The focus of this structural covariance network was especially on posterior and subcortical brain regions with less expansion into frontal brain regions. In the group early adolescence, the structural covariance network of the hippocampal tail subregion was strongly associated with thalamus, caudate, putamen, temporal pole, lingual gyrus, precuneous cortex, cerebellum vermis VIII, lateral occipital cortex, lateral occipital cortex, supramarginal gyrus, precentral gyrus, middle frontal gyrus, frontal orbital cortex,

inferior frontal gyrus (pars opercularis, pars triangularis), temporal pole, inferior temporal gyrus. In middle adolescence the structural covariance network of the tail subregion was very similar to the other groups, with large clusters of cerebellum I-IV, lingual gyrus, thalamus, intracalcarine cortex, occipital pole, precuneous cortex, caudate, putamen, frontal orbital cortex, inferior frontal gyrus (pars opercularis), middle frontal gyrus, pre- postcentral gyrus, superior parietal lobule, middle temporal gyrus (temporooccipital part), and temporal fusiform cortex.

The structural covariance network underlying the hippocampal middle body (blue) subregion consisted of pallidum, thalamus, insular cortex, central opercular cortex, Heschl's gyrus, planum polare, frontal orbital cortex, middle temporal gyrus (temporooccipital part), intra/supracalcrine cortex and cerebellum I-IV, Crus I, II, in the group of late childhood. In early adolescence, the network consisted of clusters including the cerebellum I-IV, V, temporal fusiform cortex (posterior division), middle temporal gyrus (posterior division), lateral occipital cortex (superior division), postcentral gyrus, parietal operculum cortex, middle frontal and superior frontal gyrus. In the group of middle adolescence, the structural covariance network consisted of cerebellum VII, VIII, Crus I, planum polare, central opercular cortex, frontal opercular cortex, middle temporal gyrus (posterior division), superior temporal gryus (posterior division), postcentral gyrus, temporal fusiform cortex (posterior division), frontal orbital cortex, insular cortex, superior frontal gyrus, caudate, accumbens, frontal pole, paracingulate gyrus, and supramarginal gyrus (posterior division).

In contrast to the left HS, the underlying structural covariance pattern of the right HS followed a different spatial extent for some subregions, indicating asymmetrical covariation patterns. Accordingly, the highest difference between left and right behavioral profiles of hippocampal networks was found for the medial body-tail HS associated network. While this network expanded for the left HS in the age groups of 11-14 and 15-18 years old, it remained relatively stable for the right HS indicating no specific behavioral specification. On the other hand, the tail (green) hippocampal associated structural covariance network was related to viewing, execution, and memory in the age group of 6-10 years old. But in the 15-to 18-year old group, it was behaviorally associated with navigation, memory, viewing and auditory, likely indicating an integrative role between perception and exploration behavior.

The most stable behavioral characterization was found for the anterior (yellow) subregion's network, which was persistently associated with perception (viewing, skin conductance, olfactory), emotion, cognition (memory, language) and a general automatic reactivity response (regulation, reactivity) across all three age groups.

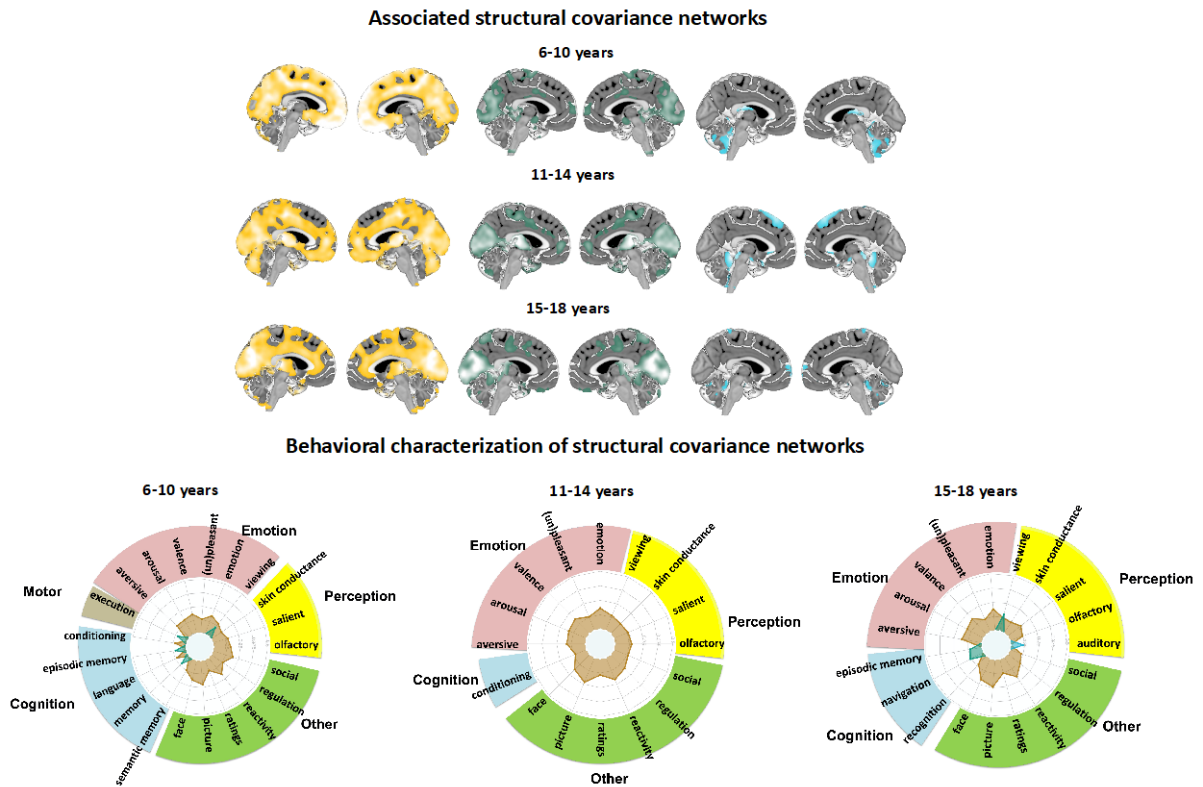


**Figure 6.** Structural covariance networks of right hippocampal differentiation pattern and their behavioral characterization.

## 2.6 Structural covariance networks underlying hippocampal differentiation pattern

We reported the unthresholded structural covariance networks associated with different hippocampal divisions, because parcellation was performed on the unthresholded structural covariance patterns of hippocampal voxels to all the other grey matter voxels in the brain. However, here, we also reported the FWE corrected structural covariance networks, which survived the statistical thresholding ( $T > 4.48$ ,  $P < 0.05$ ) (Fig. 7).

The left hippocampal anterior (yellow) subregion at the stage of late childhood was associated with a rather restricted network focused on frontal, temporal and parietal regions after statistical correction, including frontal orbital cortex, frontal pole, temporal pole, superior temporal gyrus, middle temporal gyrus, precuneous cortex, intracalcarine cortex, lingual gyrus, paracingulate gyrus, planum polare, central opercular cortex, right putamen and right pallidum. At the stage of early adolescence, the anterior subregion's networks was strongly reduced to

amygdala and precuneous cortex after statistical correction. At the stage of middle adolescence, the anterior hippocampal subregion was only associated with amygdala, cingulate gyrus posterior division and temporal pole after correction.

The structural covariance network of hippocampal tail subregion (green) was associated with the thalamus and HS CA1 in the group of late childhood after statistical correction. In the group of early and middle adolescence this network shrunk to the intracalcarine cortex, parahippocampal gyrus (posterior division), and CA1 of HS.

The structural covariance network of the middle (blue) hippocampal subregion did not survive statistical thresholding except of some voxels around the HS. In the group of early adolescence the network consisted of caudate, thalamus, accumbens, lateral occipital cortex and superior parietal lobule. In the group of middle adolescence, it consisted of the thalamus, lingual gyrus, intracalcarine cortex, pre- and postcentral gyrus and lateral occipital cortex (superior division).

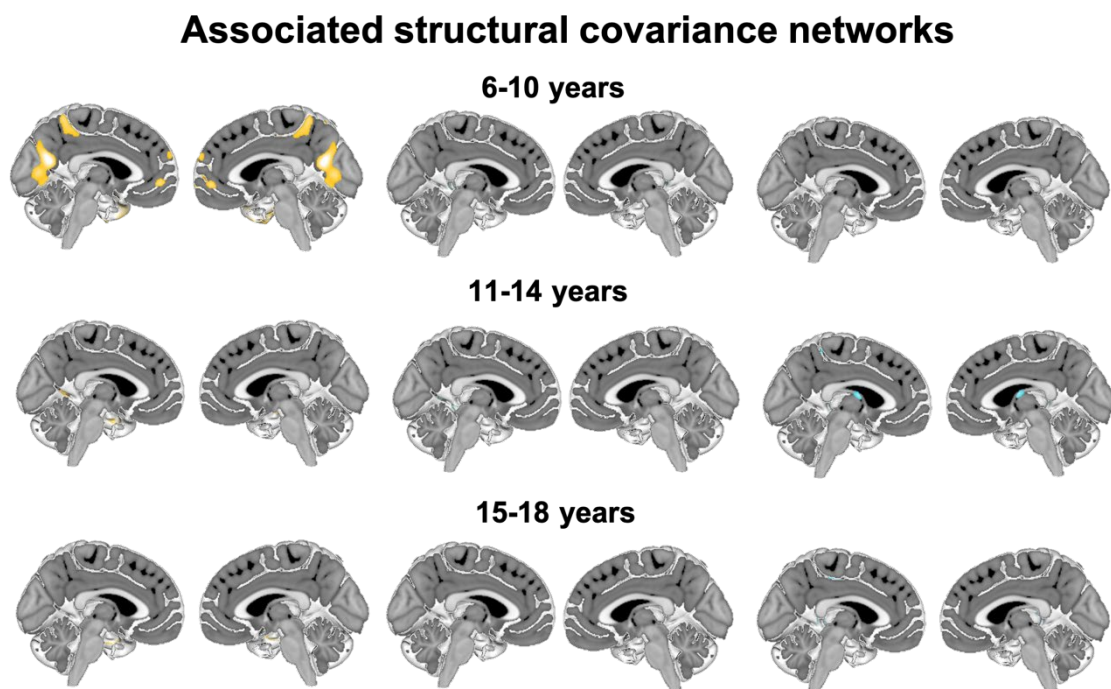


**Figure 7.** Structural covariance networks underlying the left HS division after statistical correction and thresholding.

After statistical correction, the anterior subregion of the right HS revealed associations with amygdala, parahippocampal gyrus, temporal pole, frontal pole, frontal orbital cortex, subcallosal cortex, middle frontal gyrus, inferior frontal gyrus (pars opercularis), superior

temporal gyrus (posterior division), angular gyrus and lateral occipital cortex (superior division) in late childhood. In early adolescence this network included amygdala, inferior temporal gyrus (posterior division), temporal pole, temporal fusiform cortex (posterior division), and parahippocampal gyrus (posterior division). In middle adolescence the structural covariance network consisted of amygdala, temporal fusiform cortex (posterior division), thalamus, intracalcarine cortex, cuneal cortex and temporal pole.

The tail subregion of the right HS was only associated with the thalamus after statistical correction in the group of late childhood. In early adolescence the network consisted of thalamus, inferior temporal gyrus (posterior division), temporal fusiform cortex (posterior and anterior division) and precuneous cortex. In the group of middle adolescence the hippocampal tail subregion was associated with thalamus and intracalcarine cortex.

The hippocampal middle subregion was only associated with some voxels around the HS not indicating a specific pattern after correction in the group of late childhood but was only associated with some voxels close to the HS in the temporal fusiform cortex (posterior division) in early adolescence. In the group of middle adolescence, no specific network was evident but just some voxels around the HS were associated with the hippocampal middle subregion.

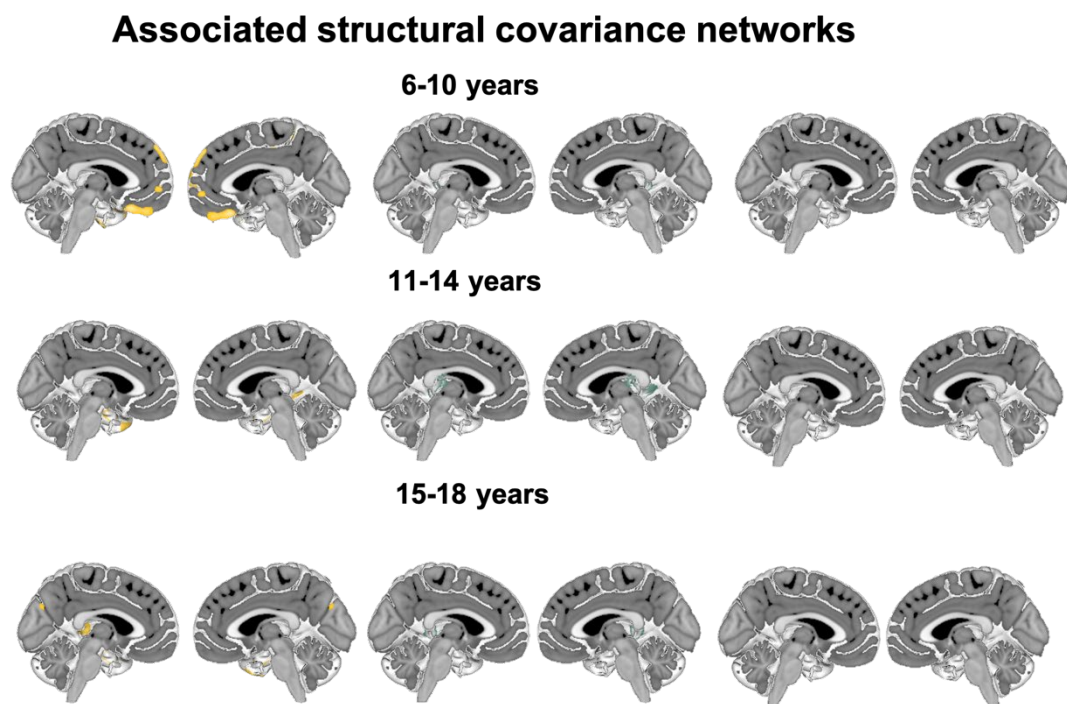


**Figure 8.** Structural covariance networks underlying the right HS division after statistical correction and thresholding.

## 2.7 Gene association profiles of structural covariance networks

Each structural covariance network related to individual hippocampal subregions was characterized by unique gene profiles supporting the assumption that hippocampal subregions are not only characterized by divergent behavioral profiles but also by divergent genetic profiles (Fig. 9).

Results of gene characterization for the right hippocampal structural covariance networks are presented in Fig. 10 with the focus on genes related to relevant domains such as ‘brain’, ‘neurons’, ‘hormones’, ‘synapses’ and ‘hippocampus’.

Overall, the gene mapping of the spatial pattern of structural covariance network of the anterior (yellow) hippocampal subregion was similar to the left HS, indicating an overall involvement in an automatic response (e.g. *FREQ* ~ circadian clock, *NTRSI* ~ blood pressure and sugar, body temperature, *MCHR2* and *THRA* ~ thyroid and melanin hormone). The gene profile of the lateral body-tail (green) hippocampal subregion’s network was even more pronounced for the right HS indicating a strong association with synaptic formation and plasticity (*NFASC* ~ synapse formation, *NPTX2* ~ excitatory synapse formation, *CHRNA2* ~ CA1 synaptic plasticity), which was especially evident for the age group of 11-14 years. The medial body-tail (blue) HS structural covariance network indicated again an involvement in an action-oriented network with motivational tendencies (e.g. *THRSP* ~ inattention, *CHRN3* ~ predisposition for tobacco dependence, *NPFF* ~ pain, reward, locomotion).

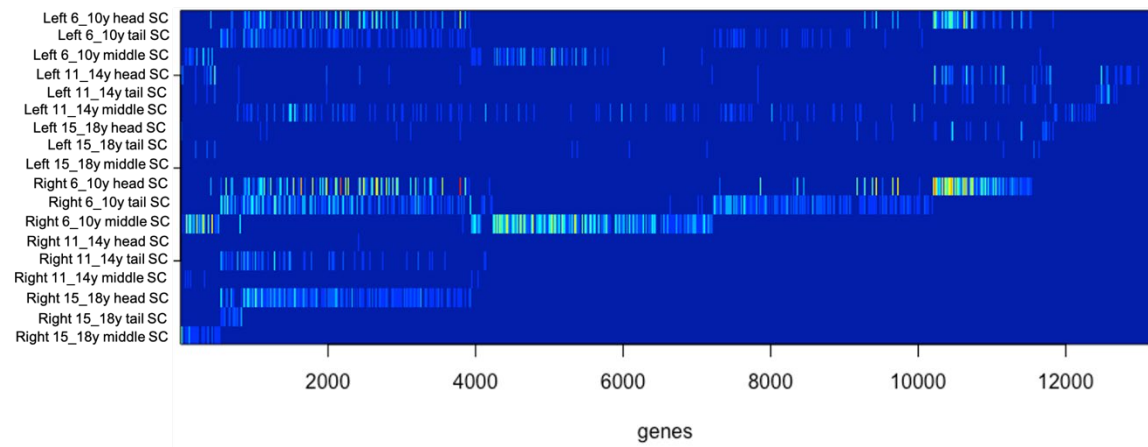
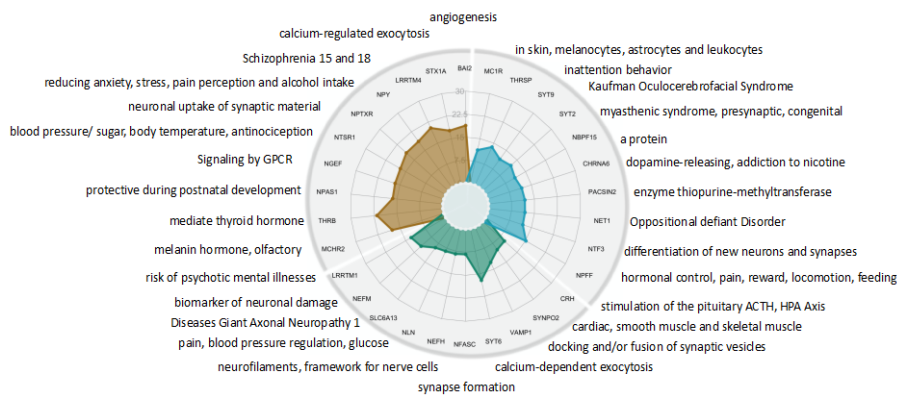


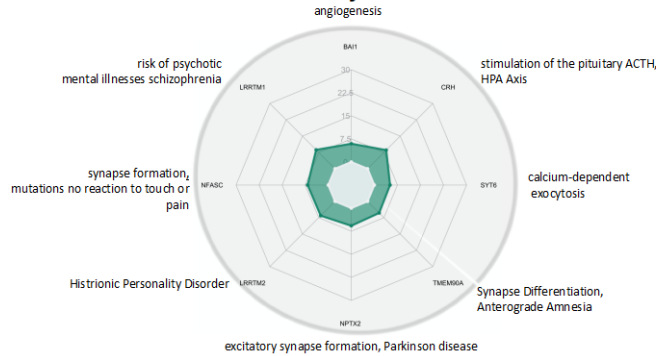
**Figure 9.** Gene profiles underlying structural covariance networks associated with each hippocampal subregion in different age groups.

## Gene profiling of structural covariance networks

### 6-10 years



### 11-14 years



### 15-18 years

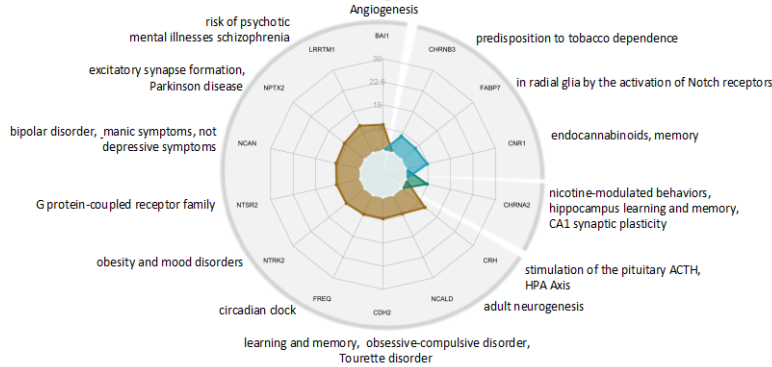


**Figure 10.** Gene mapping of structural covariance networks associated with right hippocampal differentiation pattern.